Geiger-mode operation of back-illuminated GaN avalanche photodiodes

J. L. Pau, R. McClintock, K. Minder, C. Bayram, P. Kung, and M. Razeghi[a)]
Center for Quantum Devices, Department of Electrical Engineering and Computer Science, Northwestern University, Evanston, Illinois 60208

E. Muñoz
ISOM and Departmento Ingeniería Electrónica, ETSI Telecomunicación, Universidad Politécnica de Madrid, Ciudad Universitaria s/n, Madrid 28040, Spain

D. Silversmith
Air Force Office of Scientific Research, Arlington, Virginia 22203

The authors report the Geiger-mode operation of back-illuminated GaN avalanche photodiodes. The devices were fabricated on transparent AlN templates specifically for back illumination in order to enhance hole-initiated multiplication. The spectral response in Geiger-mode operation was analyzed under low photon fluxes. Single photon detection capabilities were demonstrated in devices with areas ranging from 225 to 14063 μm^2. Single photon detection efficiency of 20% and dark count rate <10 kHz were achieved in the smallest devices. © *2007 American Institute of Physics.*
[DOI: 10.1063/1.2759980]

There is a need for single photon detectors for a variety of scientific, military, and civilian applications including free-space optical communications, quantum computing, environment monitoring, astrophysics, or biological agent detection.[1] Compared to photomultiplier tubes or superconducting single photon detectors, the use of Geiger-mode avalanche photodiodes (APDs) presents some advantages such as lower operation voltages, much reduced sizes, and no need for cooling to very low temperatures, which may enable the fabrication of more compact, lower power, and all-solid-state APD/CMOS integrated arrays.[2]

Avalanche photodiodes based on wide-band-gap semiconductors are of special interest when there is a need for reliable ultraviolet (UV) detection with single photon counting capabilities. Materials such as SiC, (Al)GaN, or diamond present optoelectrical properties with intrinsic advantages for visible-blind UV detection, potentially outperforming other narrow-band-gap counterparts that require extensive filtering. In particular, the tunable response of AlGaN detectors allows us to accomplish solar- to visible-blind performances with the same material system without the need of filters, as well as to match specific bands of biological interest within the 200–360 nm range.[3,4]

Geiger-mode operation under gated quenching has been previously demonstrated in front-illuminated GaN APDs with a single photon detection efficiency (SPDE) of 13% at a dark count rate of 400 kHz in devices with an area of 1075 μm.[2,5] However, two of the major problems with GaN APDs are the rapid increase of the dark current with area and the consequent limitation of the maximum achievable gain, which have prevented the operation of larger area devices in Geiger mode. In contrast, SiC devices have shown a low dark count rate of 28 kHz for 7854 μm^2 devices but have done this with a lower SPDE of only 3.6%.[6]

Recently, we have demonstrated that hole-initiated multiplication provides superior performance in linear mode GaN APDs due to the higher hole ionization coefficient;[8]

back-illumination maximizes the injection of holes into the multiplication region making it a better approach in *p-i-n* avalanche photodiodes. However, the realization of back-illuminated devices is more complex because of the need to minimize the underlying GaN layer thus requiring an AlGaN or AlN template and a buffer, and ruling out the use of the traditional GaN dislocation reduction strategies. In spite of these challenges, high external quantum efficiencies have been achieved in back-illuminated *p-i-n* photodiodes based on III nitrides.[8,9] In this work, we present back-illuminated GaN APDs operating in Geiger mode and review the performance of these devices.

The device structure consists of a GaN *p-i-n* homojunction grown on top of a transparent AlN template (inset of Fig. 1). The AlN is grown on a double-side polished sapphire substrate with a low-temperature AlN buffer to allow back illumination.[10] The active region consists of *p*-type GaN:Mg, unintentionally doped GaN, and *n*-type GaN:Si layers with thicknesses of 285, 200, and 200 nm, respectively.
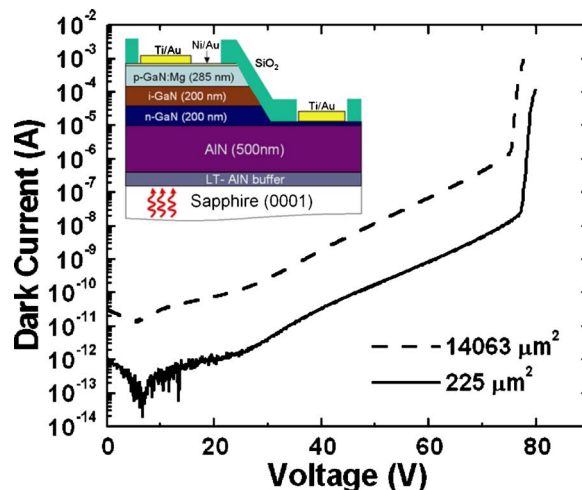

FIG. 1. (Color online) Measured *I-V* characteristics of the GaN APDs with 225 and 14063 μm^2 areas. Inset: cross-sectional diagram of the device structure

a)Electronic mail: razeghi@eecs.northwestern.edu

Capacitance-voltage measurements yielded a donor concentration of $\sim 2 \times 10^{18}$ cm^{-3} in the n-type material and a residual concentration of $\sim 2.5 \times 10^{16}$ cm^{-3} in the intrinsic layer. For the p-type GaN layer, hole concentrations of $(1-3) \times 10^{18}$ cm^{-3} were determined by Hall-effect measurements of test samples.

The devices were processed into arrays of circular detectors with areas ranging from 225 up to 14063 μm^2. A common Ti/Au (400 Å/1200 Å) n-type contact was deposited around the arrays. Ni/Au (30 Å/30 Å) thin contacts, followed by a Ti/Au (400 Å/1200 Å) bilayer were evaporated on top of each of the mesas. The entire array was then passivated with 300 nm of SiO$_2$ to help reduce the dark current and prevent premature surface breakdown.

Current-voltage (I-V) measurements were made of the different area p-i-n diodes. All devices exhibited breakdown at a reverse voltage of between 75 and 78 V. Figure 1 shows the I-V characteristics for the smallest and largest devices. The dark current for the middle size devices scaled linearly between these two curves.[11] Leakage currents at the onset of breakdown ranged from 20 nA for the 225 μm^2 area devices up to 1.6 μA for the 14063 μm^2 area devices. These values are only slightly larger than the leakage currents found in regular GaN APD structures grown on thick GaN, which are inefficient to detect UV light under back illumination.[7] The external quantum efficiency (EQE) measured at 340 nm was 9% at 0 V. To determine the EQE at higher voltages, a one-dimensional finite element model was used to estimate the photocurrent through the device as a function of bias in the absence of ionization events. This model is used to fit the experimental data at low voltages ($<$35 V), for which the ionization events are negligible, and then extrapolated to obtain the EQE values for higher voltages. This procedure estimates the EQE to be 29% just before breakdown. A similar fitting obtained from the analytical expression of the drift and diffusion currents corroborates this value.[12]

A Xe lamp and a monochromator were used to illuminate the devices within the 230–450 nm range. The light was coupled into the device through an UV fiber-optic cable. The input slit of the monochromator was adjusted to vary the photon flux, which was calibrated using a NIST traceable Si detector. The APDs were measured in Geiger mode with a gated quenching circuit, as shown in Fig. 2(a). A reverse dc voltage (V_{dc}) between 74 and 78 V was applied to the APD through a 47 kΩ resistor biasing the device just below breakdown, and a pulsed excess voltage (ΔV_p) between 8.5 and 10 V was coupled through a 50 nF capacitor to bias the device above breakdown. Pulse repetition rate was 10 kHz with a pulse width of 10 ns and a dead time of 100 μs.

The photocurrent pulses were examined using an oscilloscope to measure the voltage drop across a 50 Ω load resistor. Although 50 Ω matching cables were used, some ringing was still evident after the 10 ns pulse, primarily due to the mismatch between the device impedance and the output of the pulse generator. Figure 2(b) shows the photocurrent pulses obtained at different wavelengths in a 5625 μm^2 area device under back illumination with a flux of ten photons per pulse. For wavelengths less than the absorption cutoff, photocurrent pulses close to 0.6 mA are generated under illumination corresponding to an effective gain of about 10^7, while beyond the cutoff, a negligible photocurrent pulse is observed.
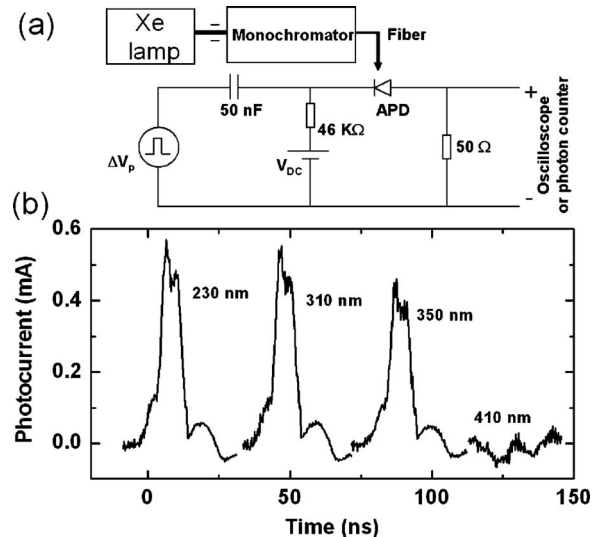

FIG. 2. (a) Gated quenching circuit and optical setup for Geiger-mode operation. (b) Photocurrent pulses obtained in a 5625 μm^2 area device at different wavelengths with a V_{dc} of 75 V and a ΔV_p of 8.5 V.

A Stanford Research model SR400 photon counter was employed to discriminate and count the photon pulses. The discriminator voltage was established to maximize the detection efficiency while minimizing the number of spurious dark counts. In order to further investigate the spectral response in photon counting mode and the uniformity of that response, four different 625 μm^2 area devices were scanned from 230 to 400 nm with a photon flux of about one photon per pulse. The average SPDE as a function of wavelength is shown with error bars in Fig. 3. Reasonably flat detection efficiency was obtained for photon energies above the band gap; below the band gap, a sharp cutoff and a high visible light rejection ratio are observed. As shown in the inset of Fig. 3, the detection cutoff is shifted to the left in comparison to the transmission cutoff, both in the unbiased case and near breakdown, under the application of 75 V reverse bias. The reason for this shift is the sharp change in the photon penetration depth close to band gap edge. Photons with energies close to the band gap have more probability of generating electron-hole pairs in the space charge region (SCR), in con-
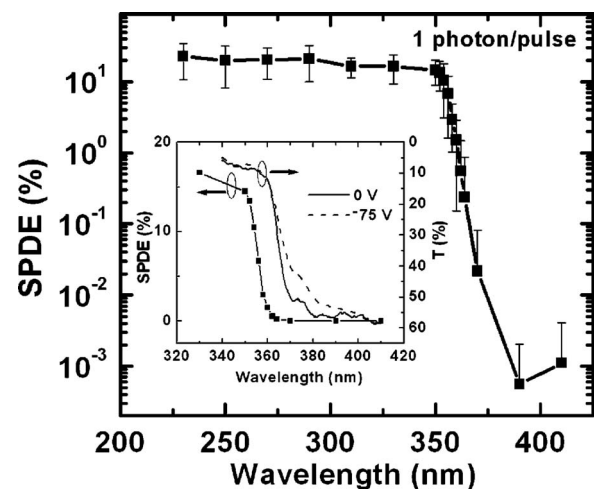

FIG. 3. Spectral response of a 625 μm^2 area device obtained at a V_{dc} of 77 V and a ΔV_p of 10 V. Inset: spectral response in linear scale and transmission measurements at 0 and -75 V.
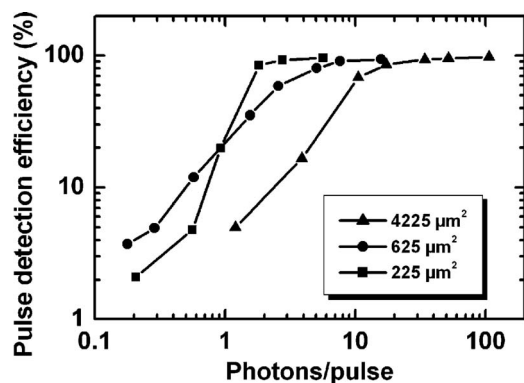
FIG. 4. Pulse detection efficiency measured as a function of photon flux for devices with 4225, 625, and 225 μm^2 areas.

FIG. 5. SPDE (left axis) and dark count rate (right axis) achieved under 340 nm illumination in devices with sizes ranging from 225 to 14063 μm^2. The straight line indicates the limit based on the maximum EQE achievable at 340 nm under bias.

trast to those with energies well above the band gap, which are more likely to be absorbed in the neutral portion of the *n*-type GaN region. The absorption of photons in the SCR increases the electron-initiated ionization in the multiplication region. Hence, the lower ionization coefficient for this type of carrier leads to smaller photocurrent pulses near the band gap, as shown in Fig. 2, for 350 nm photons. The discriminator circuit can then fail to register the smaller pulses, producing a shift in the spectral response.

It is also worthwhile to investigate the pulse detection efficiency as a function of the photon flux in order to identify the minimum photon flux for effective operation. Figure 4 shows how, as the device size increases, the photon flux needed to have a 100% probability of having a count per pulse also increases. SPDEs and dark count rates were measured in devices with areas up to 14063 μm^2. Figure 5 shows their average values obtained from measurements of three different devices for each APD area under illumination at 340 nm with a flux of one photon per pulse. The detectors with areas of 225 and 625 μm^2 presented SPDEs of 20% and 15.3%, respectively, with a dark count rate below the measurement limit (<10 kHz). Although a possible contribution from after pulsing cannot be completely ruled out, this low dark count rate suggests that the effect of thermal and tunneling processes on the pulse count is significantly reduced in the small area devices.[13]

In summary, back-illuminated GaN APDs operating in Geiger mode have been presented. These devices showed a flat Geiger-mode response for photon energies above the band gap and a high visible-light rejection ratio. Single photon counting was demonstrated in devices ranging from 225
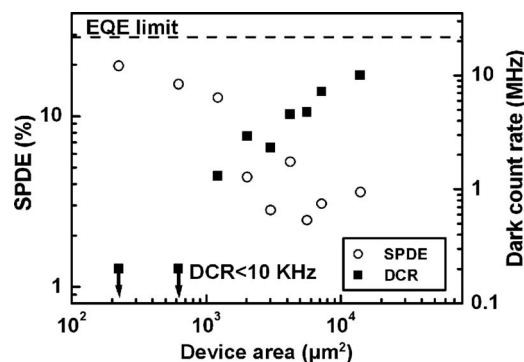
all the way up to 14063 μm^2. In the smallest device, SPDE of 20% and the dark count rate <10 kHz were obtained.

[1] I. Prochazka, K. Hamal, and B. Sopko, J. Mod. Opt. **51**, 1289 (2004).
[2] B. F. Aull, A. H. Loomis, D. J. Young, R. M. Heinrichs, B. J. Felton, P. J. Daniels, and D. J. Landers, Lincoln Lab. J. **13**, 335 (2002).
[3] M. Razeghi, A. Yasan, R. McClintock, K. Mayes, D. Shiell, S. R. Darvish, and P. Kung, Phys. Status Solidi C **1**, S141 (2004).
[4] E. Muñoz, E. Monroy, J. L. Pau, F. Calle, F. Omnès, and P. Gibart, J. Phys.: Condens. Matter **13**, 7115 (2001).
[5] K. A. McIntosh, R. J. Molnar, L. J. Mahoney, K. M. Molvar, N. Efremow, Jr., and S. Verghese, Appl. Phys. Lett. **76**, 3938 (2000).
[6] A. L. Beck, X. Guo, H.-D. Liu, A. Ghatak-roy, and J. C. Campbell, Proc. SPIE **6372**, 63720O-1 (2006).
[7] R. McClintock, J. L. Pau, K. Minder, C. Bayram, P. Kung, and M. Razeghi, Appl. Phys. Lett. **90**, 141112 (2007).
[8] R. McClintock, A. Yasan, K. Mayes, D. Shiell, S. R. Darvish, and P. Kung, Appl. Phys. Lett. **84**, 1248 (2004).
[9] C. J. Collins, U. Chowdhury, M. M. Wong, B. Yang, A. L. Beck, R. D. Dupuis, and J. C. Campbell, Electron. Lett. **38**, 824 (2002).
[10] P. Kung, R. McClintock, J. L. Pau Vizcaino, K. Minder, C. Bayram, and M. Razeghi, Proc. SPIE **6479**, 64791J-1 (2007).
[11] K. Minder, J. L. Pau, R. McClintock, P. Kung, C. Bayram, and M. Razeghi (unpublished).
[12] S. M. Sze, *Physics of Semiconductor Devices* (Wiley, New York, 1981), Chap. 13, p. 754.
[13] K. E. Jensen, P. I. Hopman, E. K. Duerr, E. A. Dauler, J. P. Donnelly, S. H. Groves, L. J. Mahoney, K. A. McIntosh, K. M. Molvar, A. Napoleone, D. C. Oakley, S. Verghese, C. J. Vineis, and R. D. Younger, Appl. Phys. Lett. **88**, 133503 (2006).